Journal of Medicinal Chemistry

pubs.acs.org/jmc

Article

Nitric Oxide Induction in Peritoneal Macrophages by a 1,2,3-Triazole Derivative Improves Its Efficacy upon *Leishmania amazonensis In Vitro* Infection

Fernando Almeida-Souza,* Verônica Diniz da Silva, Noemi Nosomi Taniwaki, Daiana de Jesus Hardoim, Ailésio Rocha Mendonça Filho, Wendel Fragoso de Freitas Moreira, Camilla Djenne Buarque, Kátia da Silva Calabrese,* and Ana Lucia Abreu-Silva

Cite This: *J. Med. Chem.* 2021, 64, 12691−12704

Read Online

ACCESS | Metrics & More | Article Recommendations | Supporting Information

ABSTRACT: 1,2,3-Triazole is one of the most flexible chemical scaffolds broadly used in various fields. Here, we report the antileishmanial activity of 1,2,3-triazole derivatives, the ultrastructural alterations induced by their treatment, and the nitric oxide (NO) modulation effect on their efficacy against *Leishmania amazonensis in vitro* infection. After the screening of eleven compounds, compound **4** exhibited better results against *L. amazonensis* promastigotes (IC_{50} = 15.52 ± 3.782 μM) and intracellular amastigotes (IC_{50} = 4.10 ± 1.136 μM), 50% cytotoxicity concentration at 84.01 ± 3.064 μM against BALB/c peritoneal macrophages, and 20.49-fold selectivity for the parasite over the cells. Compound **4** induced ultrastructural mitochondrial alterations and lipid inclusions in *L. amazonensis* promastigotes, upregulated tumor necrosis factor α, interleukin (IL)-1β, IL-6, IL-12, and IL-10 messenger RNA expressions, and enhanced the NO production, verified by nitrite (p = 0.0095) and inducible nitric oxide synthase expression (p = 0.0049) quantification, which played an important role in its activity against intramacrophagic *L. amazonensis*. *In silico* prediction in association with antileishmanial activity results showed compound **4** as a hit compound with promising potential for further studies of new leishmaniasis treatment options.

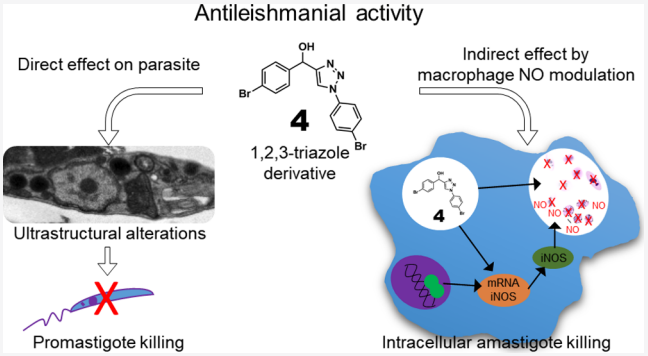

INTRODUCTION

Azoles are an important and well-known class of antifungal agent compounds. This class of drugs includes imidazoles, such as ketoconazole, and triazoles, such as fluconazole and itraconazole.[1] The mechanism of action of these drugs occurs through the inhibition of the ergosterol biosynthesis, having lanosterol 14-α-demethylase as the main molecular target, which inhibits the conversion of lanosterol to zymosterol by cytochrome P450.[1,2] Due to the presence of ergosterol as the main component of sterol in the cell membranes of *Leishmania* spp., some azoles have been studied and used for the treatment of leishmaniasis, such as ketoconazole, fluconazole, itraconazole, and posaconazole[1,3] (Figure 1).

Triazoles are heterocyclic organic compounds that are stable against metabolic degradation and capable of forming hydrogen bonds that improve their solubility and favor high affinity with biological targets.[4] 1,2,3-Triazoles gained greater prominence in organic and medicinal chemistry after the discovery of the copper-catalyzed alkyne−azide cycloaddition (CuAAC) reaction, which due to their simplicity, robustness, applicability, and versatility is a powerful tool for building active compounds with pharmacological applicability.[4,5]

Besides, the structural characteristics of 1,2,3-triazoles, such as polarity, rigidity, and the ability to act as electron donors and acceptors, allow the mimicking of different functional groups, which enhances the versatility of this class of compounds for the development of new drugs.[6] 1,2,3-Triazoles are an important medicinal scaffold with several biological properties reported, such as antibacterial,[7] anticonvulsant,[8] antiviral,[9] anticancer,[10] and anti-inflammatory activities.[11] In addition, its potential antiprotozoal activity has also been reported against the species of *Trypanosoma* and *Leishmania*.[12−14]

Leishmaniases are a group of diseases caused by *Leishmania* spp. transmitted by the bite of a parasite-infected sandfly. These

Received: April 21, 2021
Published: August 24, 2021

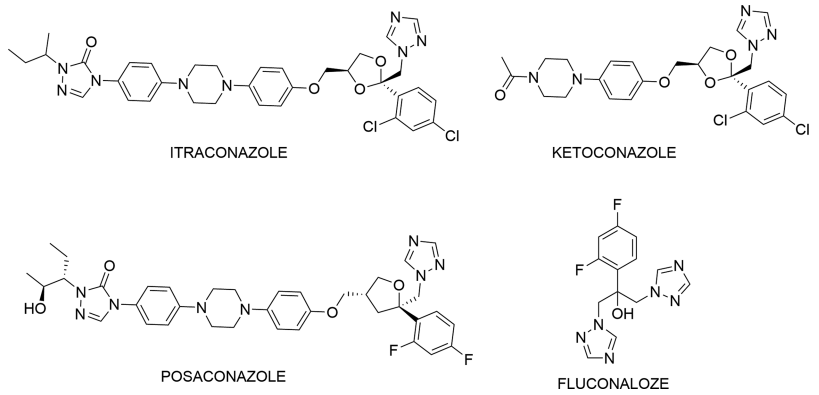

Figure 1. Chemical structure of some azole compounds with antileishmanial activity.

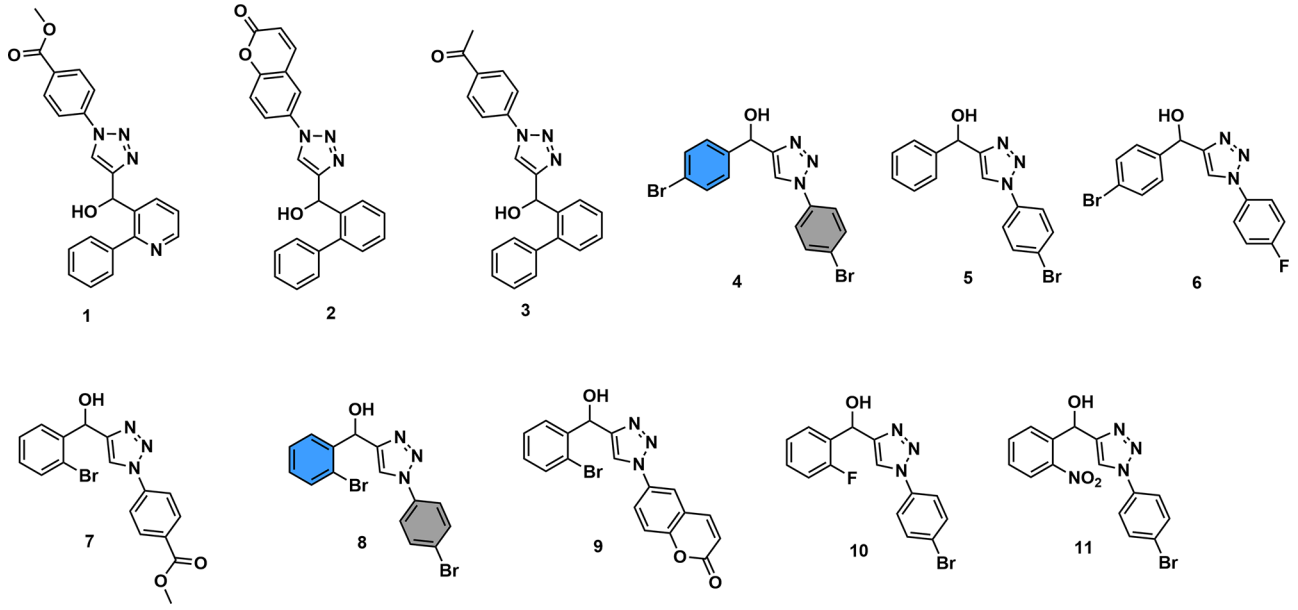

Figure 2. Chemical structure of 1,2,3-triazole derivative compounds. The highlighted compounds in blue and gray represent constitutional isomers.

diseases, widely referred to as "poor man's disease", affect millions of people worldwide and continue to be a social and economic health problem. Its current status is critical, considering the number of people at the risk of infection and emerging threats such as human immunodeficiency virus (HIV) coinfection and post-kala-azar dermal leishmaniasis.[15,16]

Leishmaniasis occurs as a spectrum of clinical features including cutaneous and visceral forms. *Leishmania amazonensis* is a species often associated with cutaneous leishmaniasis and can also cause spectral manifestations, including the mucocutaneous and visceral leishmaniasis.[17] There is no effective vaccine, and traditional treatments are toxic and expensive with a long administration duration and several adverse effects and/or drug resistance. The conventional gold standard treatment for both types is mainly intralesional or parenteral administration of antimonials, and if not treated, visceral leishmaniasis can lead to death.[18,19] Instead of treatments based only on chemotherapy, certain strategies such as chemo-immunotherapy have also focused on triggering an effective immune response by the stimulation of the cellular response and the activation of microbicidal mechanisms such as nitric oxide (NO) induction to control the parasite load.[19−21]

The emergence of strains resistant to conventional drugs, coinfections such as HIV/*Leishmania* spp., the small therapeutic arsenal (pentavalent antimonials, amphotericin B and formulations, and miltefosine), and the low investment for the discovery/development of new drugs by the pharmaceutical industry expose the urgent need for the search of new drugs with efficacy, no toxicity, and low cost against leishmaniasis.[22]

In the present study, we analyzed the *in vitro* antileishmanial activity of the 1,2,3-triazole derivative compounds, the ultrastructural alterations induced by their treatment on *L. amazonensis* promastigotes, and the effect of NO modulation induced by triazole compounds on their efficacy against *L. amazonensis in vitro* infection. We also performed an *in silico* predictive study of the physicochemical, drug-likeness, pharmacokinetics, and toxicity properties of the 1,2,3-triazole derivative compounds.

RESULTS

Antileishmanial Activity, Cytotoxicity, and Selectivity Index of 1,2,3-Triazole Derivative Compounds. For the 1,2,3-triazole derivative (Figure 2) compounds, the half-maximum inhibitory concentration against promastigotes and intracellular amastigotes of *L. amazonensis*, the cytotoxicity against BALB/c peritoneal macrophages, and the selectivity index (SI) are shown in Table 1.

https://doi.org/10.1021/acs.jmedchem.1c00725
J. Med. Chem. 2021, 64, 12691−12704

Table 1. Activity against Promastigotes and Intracellular Amastigotes of *L. amazonensis*, Cytotoxicity against BALB/c Peritoneal Macrophages, and the SI after 24 h of Treatment with 1,2,3-Triazole Derivative Compounds[a]

		L. amazonensis IC50 (μM)			
compounds	peritoneal macrophages CC_{50} (μM)	promastigotes	SI_{pro}	intracellular amastigotes	SI_{ama}
1	>400	95.85 ± 3.698	>4.17	-	-
2	140.66 ± 3.079	>200	<0.70	-	-
3	233.66 ± 4.435	56.60 ± 4.606	4.12	-	-
4	84.01 ± 3.064	15.52 ± 3.782	5.41	4.10 ± 1.136	20.49
5	>400	>200	>2.00	-	-
6	182.43 ± 3.784	45.55 ± 4.996	4.00	-	-
7	297.07 ± 3.250	27.77 ± 3.480	10.69	36.99 ± 4.142	8.03
8	312.65 ± 3.965	>200	<1.56	-	-
9	347.74 ± 3.452	81.41 ± 3.595	4.27	-	-
10	>400	110.20 ± 4.405	>3.62	-	-
11	>400	190.15 ± 4.178	>2.10	-	-
miltefosine	169.49 ± 2.982	8.02 ± 1.222	21.13	5.11 ± 1.110	33.16

[a]IC_{50}: half-maximum inhibitory concentration; CC_{50}: half-maximum cytotoxicity concentration; SI: selectivity index, obtained from CC_{50} against peritoneal macrophages/IC_{50} against promastigotes (SI_{pro}) or intracellular amastigotes (SI_{ama}); and -: not determined. Data are represented as mean ± SD and are representative of at least two experiments carried out at least in triplicate.

The assay against promastigote forms showed that compounds **4** and **7** presented better activities among the 1,2,3-triazole derivative compounds evaluated, while compounds **2**, **5**, and **8** did not present activity at the concentrations analyzed. The other compounds presented higher 50% inhibitory concentration (IC_{50}) values than miltefosine. Compounds **3**, **6**, and **7** showed median IC_{50} values against promastigotes, but compounds **3** and **6** also presented cytotoxicity, as evidenced by the SI for promastigote (SI_{pro}) values. Although compound **4** presented SI_{pro} values close to those of compounds **3** and **6**, compound **4** also presented the lowest IC_{50} values against promastigotes among these compounds. Thus, compounds **4** and **7** were selected for analysis against the intracellular amastigote forms.

Compound **4** exhibited a decrease of 3.7-fold in the IC_{50} value against intracellular amastigotes in comparison to that against IC_{50} promastigotes. On the contrary, compound **7** presented a slight loss in the antileishmanial activity when the IC_{50} value against intracellular amastigotes is compared to IC_{50} against promastigotes. The pattern of the antileishmanial activity of both compounds becomes even more evident when the concentration−response curves are analyzed with those of miltefosine. Compounds **4** and **7** presented concentration−response curves that are shifted up relative to that of miltefosine against *L. amazonensis* promastigotes (Figure 3A). For the intracellular amastigote, compound **4** displayed a concentration−response curve similar to that of miltefosine, and compound **7** displayed an even higher upward shift (Figure 3B).

The parameters of the infection analysis of *L. amazonensis*-infected cells treated with compounds **4** and **7** and miltefosine (Figure 3C−N) agreed with the results of intracellular amastigote activity, when compared with that of untreated infected cells. Compound **4** displayed a statistically low number of amastigotes per 100 cells at 40, 20, and 10 μM ($p < 0.0001$, $p < 0.0001$, and $p = 0.0495$, respectively, Figure 3D) in the same way as that of miltefosine at 40, 20, and 10 μM ($p < 0.0001$, $p < 0.0001$, and $p = 0.0004$, respectively, Figure 3F), while compound **7** only exhibited a low amastigote number at 40 μM ($p = 0.0229$, Figure 3E). Compound **4** showed less amastigotes per infected cell at 40 and 20 μM ($p = 0.0021$ and $p = 0.0140$, respectively, Figure 3H), similar to miltefosine ($p = 0.0079$ and $p = 0.0202$, respectively, Figure 3J), and compound **7** showed no alteration in this parameter even at the higher analyzed concentration (Figure 3I). For the amastigotes per cell parameter, compound **4** statistically presented low amastigote means at 40, 20, 10, and 5 μM ($p < 0.0001$, $p = 0.0001$, $p = 0.0120$, and $p = 0.0315$, respectively, Figure 3L), similar to miltefosine ($p = 0.0001$, $p = 0.0023$, $p = 0.0011$, and $p = 0.0216$, respectively, Figure 3L), and compound **7** only exhibited a low amastigote mean at 40 μM ($p = 0.0357$, Figure 3E). The effect of treatment with compounds **4** and **7** and miltefosine on *L. amazonensis*-infected cells can be visually observed in the photomicrograph images (Figure 3O).

The cytotoxicity analysis was performed against the human fibroblast cell line CCD-1072Sk and BALB/c peritoneal macrophages. The eleven 1,2,3-triazole derivative compounds did not display cytotoxicity against CCD-1072Sk cells at concentrations below 400 μM, the highest concentration analyzed by us, while miltefosine showed a 50% cytotoxicity concentration (CC_{50}) of 190.85 ± 1.147 μM. CC_{50} values of peritoneal macrophages treated with 1,2,3-triazole derivative compounds are shown in Table 1. As 1,2,3-triazole derivative compounds did not show cytotoxicity against fibroblasts, cytotoxicity against peritoneal macrophages was used to determine the selectivity index (SI) values. Compound **4** presented higher toxicity against peritoneal macrophages among the 1,2,3-triazole derivative compounds evaluated. However, as compound **4** also displayed better activity against *L. amazonensis* intracellular amastigotes, it presented an SI higher than that of compound **7**, demonstrating that it was more toxic to the intracellular amastigotes than to the macrophage.

Ultrastructural Changes in *L. amazonensis* Promastigotes Induced by 1,2,3-Triazole Derivative Compounds. The 1,2,3-triazole derivative compounds **4** and **7** that demonstrated better activity against *L. amazonensis* promastigote forms were evaluated for ultrastructural alterations induced by its treatment. Parasites with a normal elongated morphology and no alterations in organelles are shown in Figure 4A. Electron-dense corpuscles characteristic of lipid inclusions, small vesicles surrounded by a membrane in the cytoplasm, and some membrane profiles near the flagellar pocket were observed in parasites treated with compounds **7** (Figure 4B−D) and **4** (Figure 5A−D). Compound **4** also showed parasites with kinetoplast swelling (Figure 5B−D).

https://doi.org/10.1021/acs.jmedchem.1c00725
J. Med. Chem. 2021, 64, 12691−12704

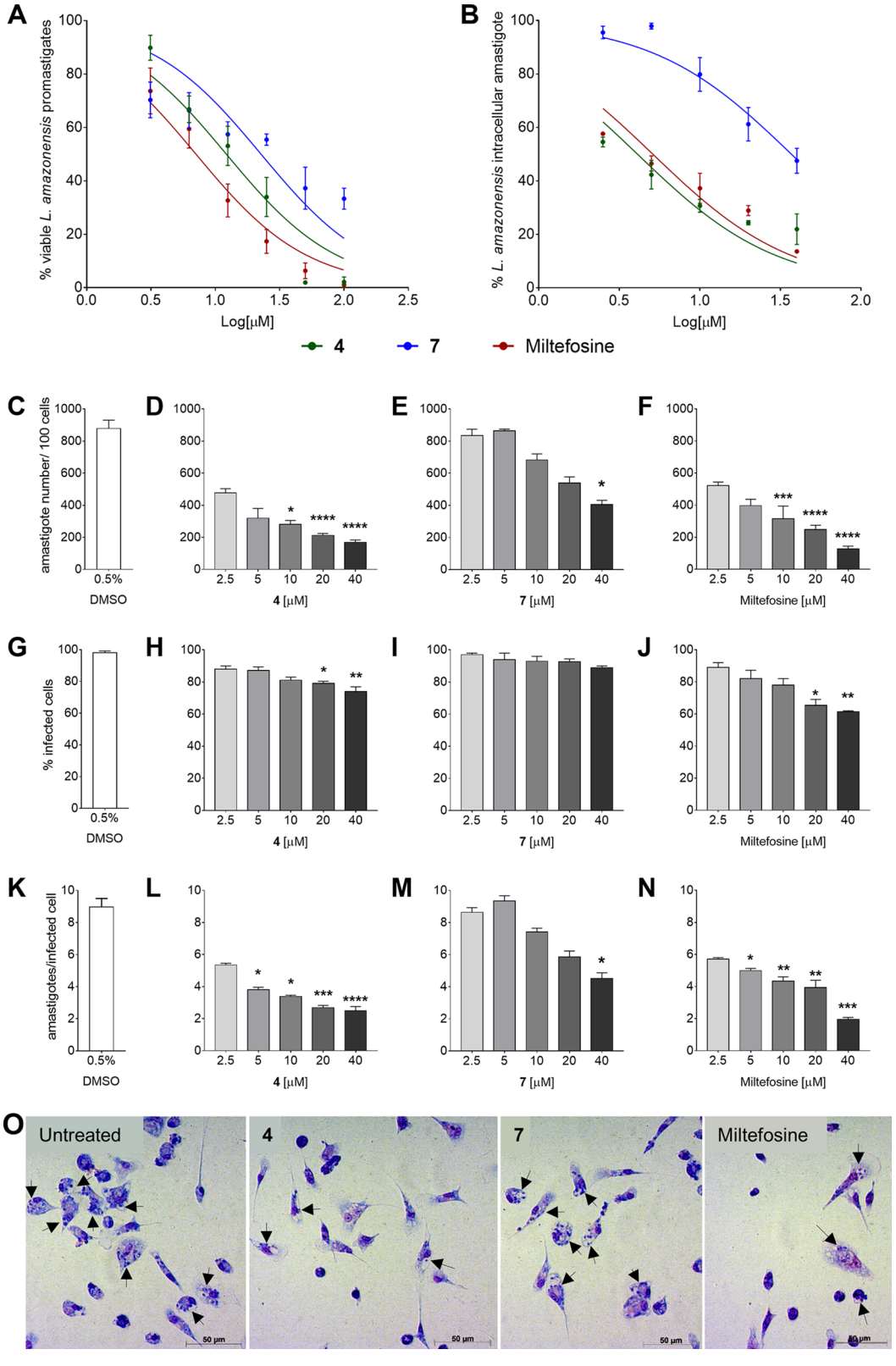

Figure 3. *In vitro* effects of 1,2,3-triazole derivative compounds **4** and **7** against *L. amazonensis*. Concentration−response curves against promastigote (A) and intracellular amastigote forms (B), parameters of infection (C−N), and light microscopy (O) of *L. amazonensis*-infected peritoneal macrophages after 24 h of treatment. Data are represented as mean ± SD and are representative of at least three independent experiments carried out at least in triplicate. *$p < 0.05$, **$p < 0.01$, ***$p < 0.001$, and ****$p < 0.0001$ when compared with the control group treated with 0.5% dimethyl sulfoxide (DMSO) by the Kruskal−Wallis test and post hoc Dunn's test. Images are representative of two independent experiments carried out at least in triplicate of *L. amazonensis*-infected cells treated with DMSO 0.5% or compounds **4** and **7** and miltefosine at 5 μM. Arrows point to amastigotes within macrophages. Giemsa, 20× objective.

https://doi.org/10.1021/acs.jmedchem.1c00725
J. Med. Chem. 2021, 64, 12691−12704

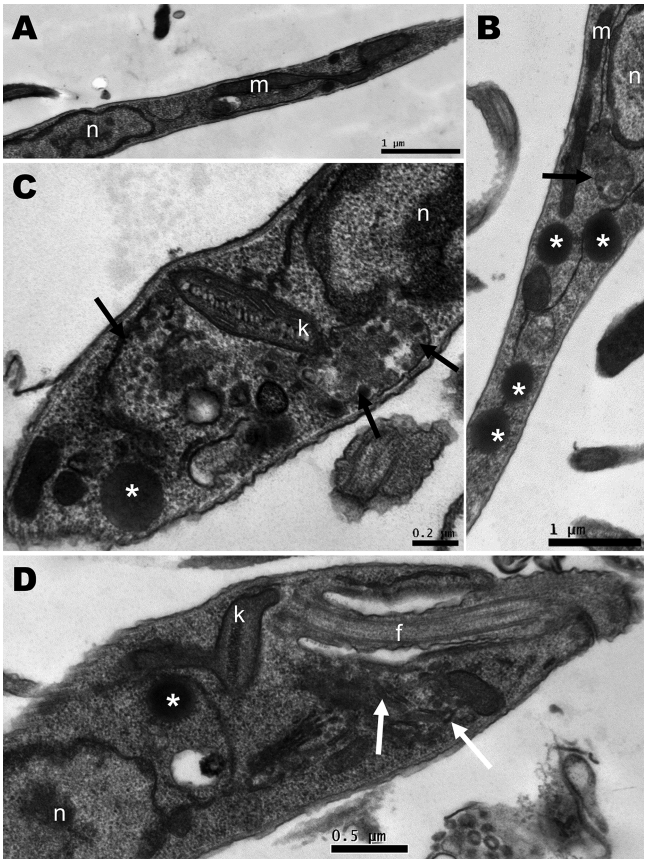

Figure 4. *L. amazonensis* promastigote ultrastructure observed by transmission electron microscopy. (A) Control parasites treated for 24 h with DMSO 0.5%. (B–D) Parasites treated for 24 h with the 1,2,3-triazole derivative compound **7** at 27.77 μM displayed lipid inclusions (white asterisks) and small vesicles surrounded by a membrane (B) or with the involvement of the endoplasmic reticulum (C) in the cytoplasm (arrows) and profiles of membranes near the flagellar pocket (white arrows) (D). n: nucleus, m: mitochondrion, k: kinetoplast, and f: flagellum.

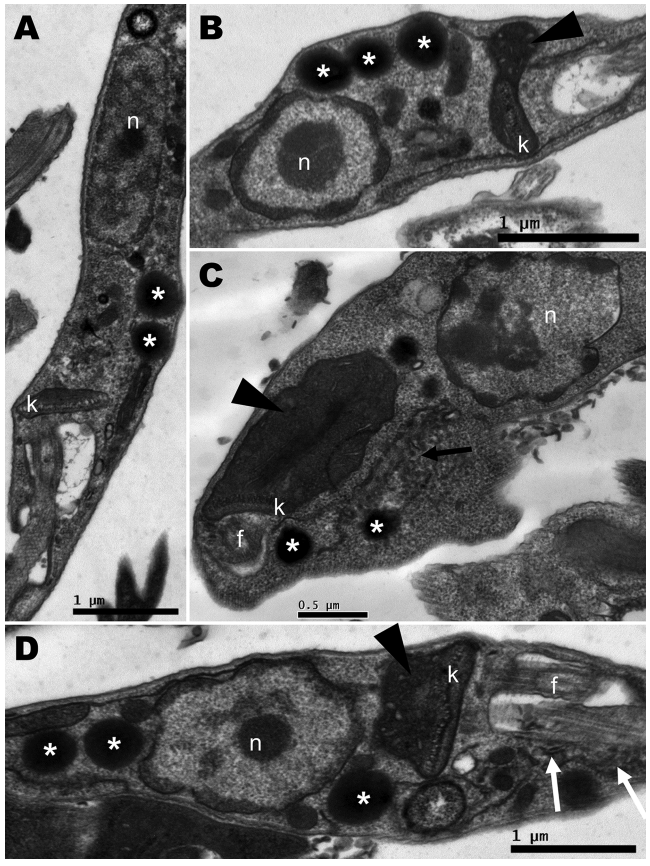

Figure 5. Ultrastructural changes of *L. amazonensis* promastigote forms treated for 24 h with the 1,2,3-triazole derivative compound **4** at 15.52 μM. (A–D) Lipid inclusions (white asterisks). Vesicles and some membrane profiles surrounded by the endoplasmic reticulum (arrows) and near the flagellar pocket (white arrows) and kinetoplast swelling with irregular cristae (arrowhead) (C,D). n: nucleus, k: kinetoplast, and f: flagellum.

1,2,3-Triazole Derivative Compound Modulates NO Production and Cytokine Expression in Peritoneal Macrophages. The 1,2,3-triazole derivative that presented better activity against intracellular amastigotes, compound **4**, was submitted to the evaluation of NO modulation in peritoneal macrophages. The cells treated for 48 h with compound **4** showed high levels of nitrite at 50 μM (4.63 ± 1.801 μM $NaNO_2$, $p = 0.0420$) and 100 μM (4.34 ± 1.593 μM $NaNO_2$, $p = 0.0294$) compared to untreated cells (3.22 ± 0.570 μM) (Figure 6A). However, compound **4** at 100 μM showed a decreased viability of 65.79 ± 5.599% in relation to untreated cells (Figure 6B); thus, posterior assays were carried out with compound **4** at 50 μM. When compared to those of uninfected and untreated cells (5.77 ± 0.308 μM $NaNO_2$), nitrite levels were lower in *L. amazonensis*-infected and untreated cells (4.11 ± 0.156 μM $NaNO_2$, $p = 0.0286$). However, nitrite levels in *L. amazonensis*-infected cells treated with compound **4** (9.37 ± 2.003 μM $NaNO_2$) were significantly higher ($p = 0.0095$) than nitrite levels in untreated and infected cells (Figure 6C). Nitrite quantification was corroborated by inducible nitric oxide synthase (iNOS) messenger RNA (mRNA) expression quantification. Treatment with compound **4** upregulated iNOS mRNA expression in uninfected cells (12.28 ± 1.289-fold, $p = 0.0040$) and in *L. amazonensis*-infected cells (24.47 ± 6.375-fold, $p = 0.0049$) (Figure 6D). The 1,2,3-triazole derivative treatment was able to induce the same pattern observed for iNOS mRNA expression in the other cytokines evaluated. Tumor necrosis factor α (TNF-α, Figure 6E) and interleukin (IL)-1β (Figure 6F) presented similar mRNA expression upregulation to that of iNOS, while IL-6 (Figure 6G), IL-12 (Figure 6H), and IL-10 (Figure 6I) showed slightly lower upregulation than iNOS and the other two cytokines.

Antileishmanial Activity of the 1,2,3-Triazole Derivative Compound Is Decreased by iNOS Inhibition. To evaluate the role of NO induction in the antileishmanial activity of the 1,2,3-triazole derivative compound **4**, we selectively inhibited iNOS with *N*-(3-(aminomethyl)benzyl)acetamidine dihydrochloride (1400W, Figure 7A). First, we quantified nitrite to ensure that 1400W was able to decrease the nitrite levels in our treatment conditions (Figure 7B). It was verified once again that *L. amazonensis* infection induced a reduction in the nitrite levels (2.60 ± 0.236 μM $NaNO_2$; $p = 0.0370$) compared to that of uninfected and untreated cells (4.27 ± 0.432 μM $NaNO_2$), and the treatment of infected cells with 1400W reduced this level even more (2.06 ± 0.410 μM $NaNO_2$, $p = 0.0068$). Then, we verified that 1400W successfully decreased nitrite levels in uninfected cells treated with compound **4** (2.65 ± 0.694 μM $NaNO_2$, $p = 0.0007$) and in *L. amazonensis*-infected cells treated with compound **4** (3.06 ± 0.236 μM $NaNO_2$, $p = 0.0002$). Next,

https://doi.org/10.1021/acs.jmedchem.1c00725
J. Med. Chem. 2021, 64, 12691–12704

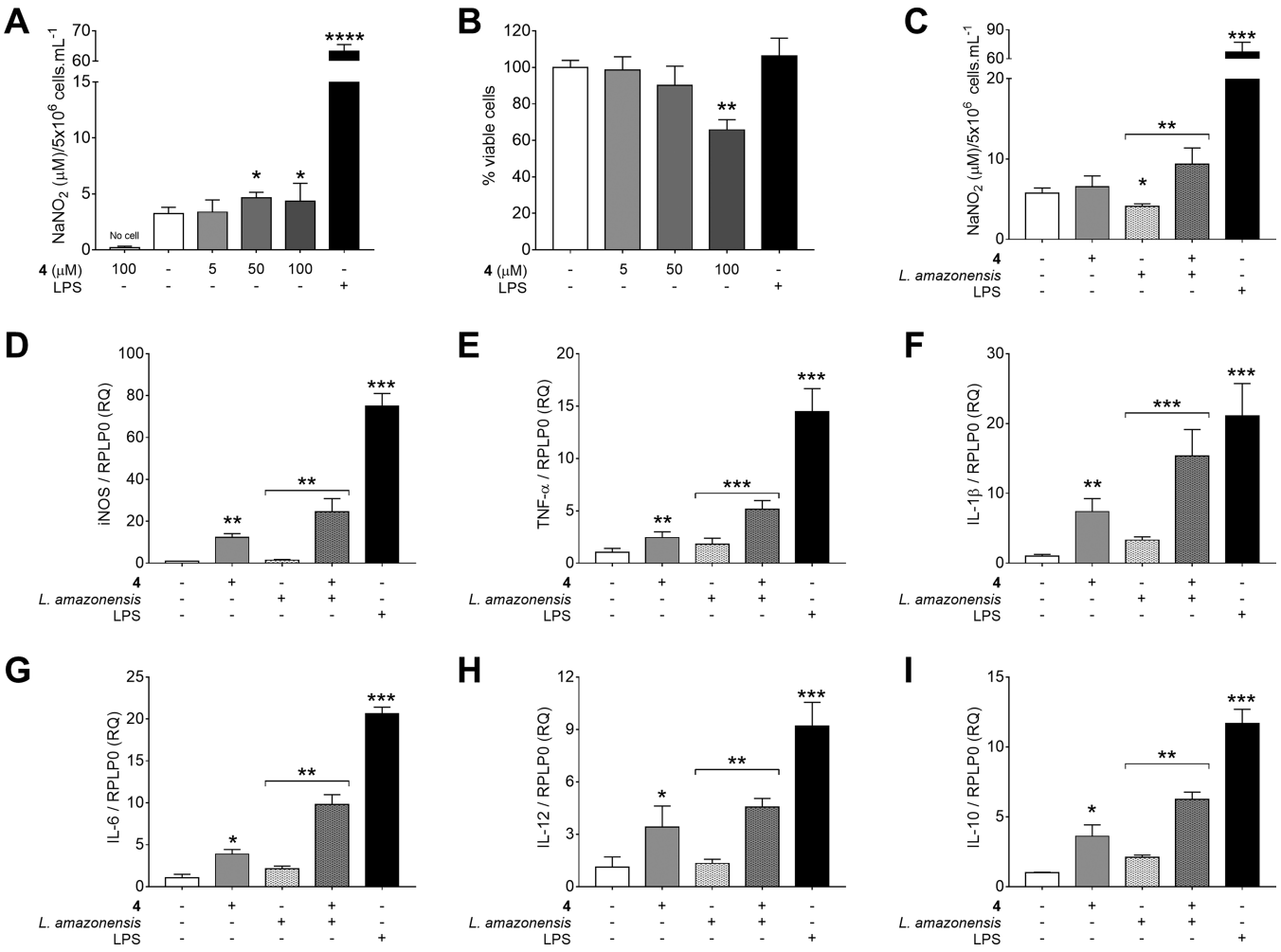

Figure 6. 1,2,3-Triazole derivative compound **4** increases NO production. Nitrite quantification (A) and viability (B) of BALB/c peritoneal macrophages treated with compound **4** or LPS at 10 μg/mL for 48 h. Quantification of nitrite (C) and mRNA expression of iNOS (D), TNF-α (E), IL-1β (F), IL-6 (G), IL-12 (H), and IL-10 (I) of *L. amazonensis*-stimulated cells treated with compound **4** at 50 μM for 48 h. iNOS: inducible nitric oxide synthase; TNF: tumor necrosis factor; IL: interleukin; RPLP0: ribosomal protein lateral stalk subunit P0; and RQ: relative quantification. Data are represented as mean ± SD and are representative of two independent experiments carried out at least in triplicate. *$p < 0.05$, **$p < 0.01$, ***$p < 0.001$, and ****$p < 0.0001$ when compared with the control group untreated and unstimulated or between brackets by the Mann−Whitney test.

we evaluated the parameters of infection after the treatment with 1400W (Figure 7C−E). Cells treated with 1400W and compound **4** exhibited an enhancement in all three parameters of infection, with the number of amastigotes per 100 cells (288.25 ± 8.098, $p = 0.0159$, Figure 7C), percentage of infected cells (79.6 ± 3.286, $p = 0.0397$, Figure 7D), and amastigotes per cells (3.68 ± 0.0933, $p = 0.0238$, Figure 7E) exhibiting high values when compared to those of cells treated with compound **4** and untreated with 1400W (169.38 ± 32.33, 55.6 ± 5.367, and 2.86 ± 0.421, respectively). These results indicate that NO production plays an important role in the 1,2,3-triazole derivative compound **4** activity against *L. amazonensis* intracellular amastigotes.

Prediction of *In Silico* Physicochemical, Drug-Likeness, Pharmacokinetics, and Toxicity Properties of 1,2,3-Triazole Derivative Compounds. The *in silico* physicochemical (Table S1), drug-likeness (Table S2), medicinal chemistry (Table S3), and pharmacokinetics and toxicity (Table S4) properties were predicted for the 1,2,3-triazole derivative compounds synthesized. Drug-likeness property rules, Lipinski's rule of five and Veber, Ghose, Muegge, and Egan rules were applied to the compounds, which demonstrated that all analyzed compounds obeyed all the rules. In medicinal chemistry property prediction, pan-assay interference compounds (PAINS) analysis did not identify any alert of problematic fragments, while Brenk filters created alerts to compounds **2**, **8**, and **10**. Leadlikeness prediction identified alerts to all compounds except compounds **5** and **6**. Compounds **4** and **7** presented alerts to molecular weight higher than 350. All compounds presented easy synthetic accessibility prediction. The graphical output of SwissADME prediction is presented for compounds **4** and **7**, which exhibited the best antileishmanial activity (Figure 8). In the bioavailability radar of drug-likeness properties, both compounds presented prediction values inside the ideal rage for lipophilicity, size of molecule, polarity, solubility, and flexibility but not for the saturation parameter (Figure 8A). The boiled-egg graphic showed that compound **4** presented blood−brain barrier (BBB) permeability and high human intestinal absorption (HIA) but is not P-glycoprotein substrate (Figure 8B). *In silico* pharmacokinetics properties were predicted for compounds **4** and **7** with the pkCSM tool that reinforced the SwissADME results. Briefly, compound **4** displayed high intestinal absorption, readily crossed the BBB, presented as P-glycoprotein non-substrate, and also revealed low

https://doi.org/10.1021/acs.jmedchem.1c00725
J. Med. Chem. 2021, 64, 12691−12704

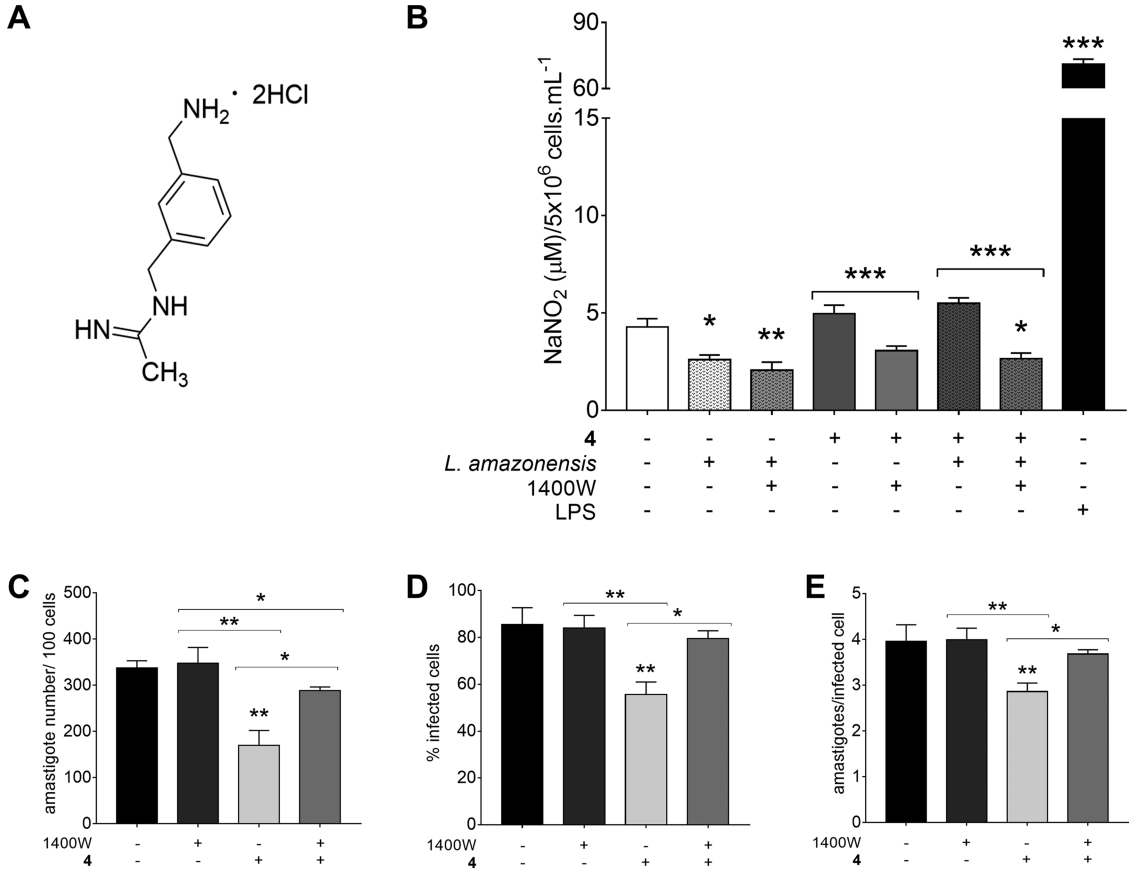

Figure 7. iNOS inhibition decreases the leishmanicidal activity of the 1,2,3-triazole derivative compound **4**. (A) Chemical structure of 1400W. (B) Nitrite quantification in the supernatant of BALB/c peritoneal macrophages pretreated with 1400W at 200 nM, stimulated with *L. amazonensis* or LPS at 10 μg/mL, and treated with compound **4** at 50 μM for 48 h. (C–E) Parameters of infection of *L. amazonensis*-infected cells pretreated with 1400W at 200 nM and treated with compound **4** at 15.52 μM for 24 h. Data are represented as mean ± SD and are representative of two independent experiments carried out at least in triplicate. *$p < 0.05$, **$p < 0.01$, and ***$p < 0.001$, when compared with the untreated group or between brackets by the Mann–Whitney test.

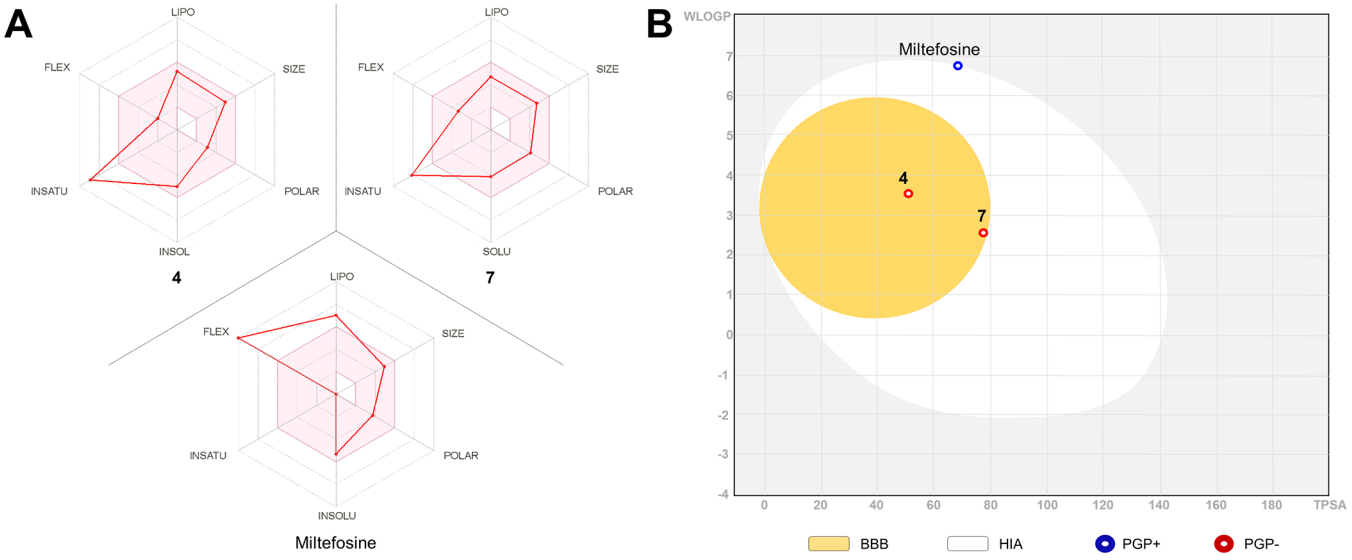

Figure 8. SwissADME graphical output of 1,2,3-triazole derivative compounds. (A) Bioavailability radar of drug-likeness where the pink area characterizes the ideal range for the properties lipophilicity (LIPO), size (SIZE), polarity (POLAR), solubility (INSOLU), saturation (INSATU), and flexibility (FLEX). (B) Boiled-egg graphic where compounds inside the yolk indicate access through the blood–brain barrier (BBB) and inside white indicate human intestinal absorption (HIA) and blue or red dots represent prediction to the P-glycoprotein substrate (PGP+) or P-glycoprotein non-substrate (PGP–), respectively.

https://doi.org/10.1021/acs.jmedchem.1c00725
J. Med. Chem. 2021, 64, 12691–12704

skin permeability, metabolization by different isoforms of cytochrome P450, and excretion as a renal organic cation transporter 2 substrate. Toxicity prediction of compounds **4** and **7** showed no hepatotoxicity, skin sensitization, or inhibition of human ether-a-go-go I and II and no mutagenic or carcinogenic potential according to the *Salmonella*/microsome mutagenicity assay.

DISCUSSION

In the light of our knowledge, we report here for the first time the effect of NO induction by 1,2,3-triazole derivative compounds on the *in vitro* activity against intracellular amastigotes of *L. amazonensis*. Initially, we showed the antileishmanial activity of 1,2,3-triazole derivative compounds against the promastigote forms of *L. amazonensis* and described the ultrastructural alterations caused by this treatment.

There are no literature data about the *in vitro* activity of 1,2,3-triazole derivatives against *Leishmania*; however, previous studies have reported the leishmanicidal activity of several 1,2,3-triazole derivatives.[13,23] Compounds **4** and **7** were the two triazole derivatives that presented the best activity. In addition to the triazole group of compounds **4** and **7**, the presence of halogens such as bromine also favors the pharmacological activity due to the halogen bonds with a carbonyl, hydroxyl, charged carboxylate, or phosphate group of biomolecules stabilizing inter- and intramolecular interactions that are important for ligand binding and molecular folding.[24]

Compounds **4** and **8** are constitutional isomers, with the bromine atom in different positions in the aromatic ring (blue ring, Figure 2). However, while compound **8** was inactive, compound **4** presented the best antileishmanial activity among the compounds evaluated. It is not uncommon since some other isomers of 1,2,3-triazole analogues also show different biological activities,[25,26] including against *L. amazonensis*,[27] highlighting the need for their evaluation to ensure their activity, as observed in this work.

Regarding the presence of the halogen, the difference in the antileishmanial activities against the promastigote forms is due to the position of the halogen in the aromatic ring and not just its presence. This fact is common in medicinal chemistry where isomers display differences in biological activities. For instance, different halogen atom positions cause distinct distributions of the halogen bond that may alter its interactions between the enzyme substrates and consequently its substrate selectivity of enzymatic catalysis.[28]

The promastigote activity observed for compounds **4** and **7** indicates their direct action on the parasite. This direct action was evidenced by the ultrastructural changes detected by transmission electron microscopy of *L. amazonensis* promastigotes. Treatment with compounds **4** and **7** induced alterations such as an increase of lipid inclusions associated with the vesicles due to the presence of vesicles and membrane profiles surrounded by the endoplasmic reticulum in the cytoplasm and near the flagellar pocket. These changes were also observed in parasites treated with compounds that alter the lipid biosynthesis, such as 22,26-azasterol, a delta(24(25))-sterol methyltransferase inhibitor,[29] and 1,4-disubstituted-1,2,3-triazole compounds,[13] inducing lipid bodies and vesicle accumulation in the cytoplasm. These cytoplasmic structures indicate an increase in the exocytic activity in the region of the flagellar pocket as an attempt to secrete the abnormal lipids.[30] The presence of profiles of the endoplasmic reticulum forming vacuoles containing vesicles and membranes and the loss of this organelle integrity may be a consequence of the drug action. The treatment with compound **4** also induced mitochondrial/kinetoplast swelling, an alteration observed in *Leishmania* treated with other triazole derivatives.[13,31] The mitochondrial swelling in *L. amazonensis* promastigotes may be related to its dysfunction due to the increment in reactive oxygen species and the depolarization of the mitochondrial membrane potential induced by 1,2,3-triazole derivatives.[12]

The cytotoxicity of 1,2,3-triazole derivatives was evaluated against CCD-1072Sk fibroblast cells and BALB/c peritoneal macrophages, however, no fibroblast cytotoxicity was observed for any of the triazole compounds analyzed. Low cytotoxicity was also observed in other triazole compounds that displayed CC_{50} higher than 500 μM on mammalian cells.[32] It is well-known that cytotoxicity depends on the type of cell line, and in general, fibroblast cells exhibit more resistance than macrophages.[33,34] In cytotoxicity against peritoneal macrophages, compound **4** presented the highest cytotoxicity among them. In order to evaluate the influence of halogens and increase the liposolubility of compound **4**, a substitution of bromine by fluorine was made, generating compounds **6** and **10**. Drug fluorination is commonly used to enhance membrane permeation and to increase liposolubility, allowing them to pass through lipid membranes.[35,36] The absence of bromine in one of the rings in compound **5** was also evaluated. Compounds **5**, **6**, and **10** had decreased cytotoxicity compared to compound **4**; however, these compounds also exhibited a decreased activity against promastigotes compared to compound **4**.

Although the *in vitro* activity against promastigotes is used in several studies as a screening assay for new compounds against leishmaniasis, its result alone cannot be considered as a parameter to classify a compound as having antileishmanial potential. Activity against the intracellular amastigotes is the proper way to show a relationship between the *in vitro* activity of a compound with possible efficiency *in vivo*.[21] In addition, there are recommendations of global initiatives, such as the Drugs for Neglected Diseases Initiative (DNDi) and the Pan-Asian Screening Network, whereupon promising antileishmanial compounds should feature IC_{50} lower than 10 μM.[37] Thus, we chose the two compounds that presented the lower IC_{50} values against promastigotes and the higher SI_{pro}, compounds **4** and **7**, to evaluate their activity against *L. amazonensis* intracellular amastigotes. Comparing their activity against promastigotes to their activity against intracellular amastigotes, compound **4** exhibited an increase in the activity, while compound **7** showed a slight decrease.

The activity exhibited by compound **4** against intracellular amastigotes associated with the low cytotoxicity against BALB/c peritoneal macrophage resulted in the highest SI value among the compounds evaluated, demonstrating that compound **4** is more selective to the parasite than being toxic to mammal cells. The SI is a widely used criterion for the identification of potential new drugs by global initiatives such as the DNDi and the Japanese Global Health Innovative Technology, which define that the SI of a hit or lead compound should be greater than 10-fold.[13,38] As compound **4** obeys this criterion, presenting an SI of 20.49, it can naturally be classified as a hit compound.

The increase in the antileishmanial activity observed for compound **4**, comparing promastigote and intracellular amastigote assays results, might be a suggestion of an indirect mechanism of action on infected cells, in addition to the direct action on promastigote forms also detected by transmission

https://doi.org/10.1021/acs.jmedchem.1c00725
J. Med. Chem. 2021, 64, 12691−12704

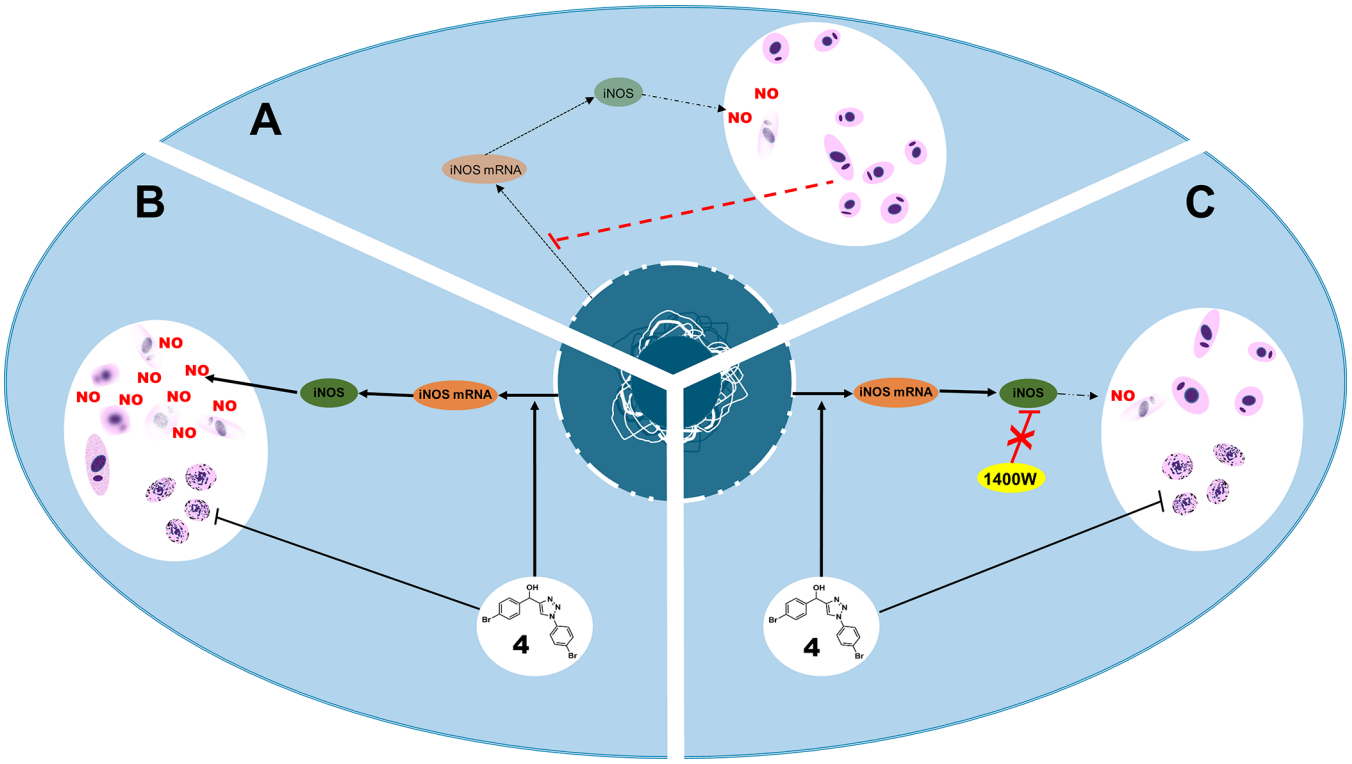

Figure 9. Role of nitric oxide (NO) in the *in vitro* antileishmanial activity of compound **4**. (A) *L. amazonensis* parasites downregulate inducible nitric oxide synthase (iNOS) expression, decreasing NO production. (B) Compound **4** directly kills *L. amazonensis* parasites and induces NO production by upregulation of iNOS expression, leading to an improvement of microbicidal action by macrophages and enhancing compound **4** antileishmanial activity. (C) 1400W inhibits iNOS, decreasing NO production and defeating NO modulation by compound **4**, which exhibits only a direct activity that is lower than its combined direct and indirect activity on *L. amazonensis*, leading to an increase in the parasite load inside macrophages.

electron microscopy. There are several forms of a molecule that indirectly act against intracellular parasites, NO induction being one of the most effective,[39,40] especially against *Leishmania*.[41,42] NO acts on pathogenic microorganisms by the inhibition of proliferation, induction of DNA mutagenesis, disruption of [FeS] clusters, metabolic blockade, and inactivation of virulence factors.[21,43] Therefore, we evaluated the role of NO induction in macrophages treated with compound **4**.

1,2,3-Triazole is the most flexible chemical scaffold and has been broadly used in various fields. Triazole derivative compounds have been described to be both acting as an anti-inflammatory, inhibiting NO and other pro-inflammatory markers,[44,45] and acting as a NO donor[46] or as pro-inflammatory molecules, inducing an increase in the NO production.[13] We observed that compound **4** induced NO production in BALB/c peritoneal macrophages whether infected or not with *L. amazonensis*, detected both by nitrite quantification in the culture supernatant and by iNOS mRNA expression. The maintenance of the induction of NO production and iNOS expression even in infected macrophages may characterize this as one of its effector mechanisms against *L. amazonensis* intracellular amastigotes.

There are three known NOS isoforms often described by their tissue-specific expression patterns: neuronal NOS (nNOS or NOS1) in the neuronal tissue; inducible NOS (iNOS or NOS2), which is upregulated in activated macrophages by various pro-inflammatory factors such as cytokines or endotoxins; and endothelial NOS (eNOS or NOS3) in the endothelium where it regulates the vascular tone.[47,48] Thus, to evaluate the effects of compound **4** in NO generation and its role in leishmanicidal activity, we used the selective iNOS inhibitor N-(3-(aminomethyl)benzyl) acetamidine dihydrochloride, commonly denominated as 1400W.

1400W is a tight binding, irreversible or extremely slow reversible inhibitor of iNOS. 1400W was at least 5000-fold selective for iNOS versus eNOS in humans, and it was greater than 50-fold potent against iNOS than eNOS in a rat model.[49] As expected, 1400W reduced nitrite levels in all situations used in our experiments: on *L. amazonensis* infection or not; on treatment with compound **4** or not; and on *L. amazonensis* infection and compound **4** treatment. Consequently, it was possible to evaluate the role of NO in the leishmanicidal activity of compound **4** through the pharmacological inhibition of the iNOS enzyme by 1400W.

The infection assay with iNOS inhibition by 1400W demonstrated the importance of increased NO production induced by the treatment with compound **4**. In*L. amazonensis* infected peritoneal macrophages treated with 1400W, compound **4** exhibited more intracellular amastigotes than those treated only with compound **4**, and all the parameters of infection were almost similar to those of untreated and infected cells. This clearly shows that the induction of NO production by macrophage activation plays an important role in compound **4** activity against intracellular amastigotes of *L. amazonensis* and that NO inhibition resets the infection to a condition nearly similar to that of infected and untreated macrophages (Figure 9).

Besides inducing iNOS mRNA expression, compound **4** also upregulated the expression of the pro-inflammatory cytokines TNF-α, IL-1β, IL-6, and IL-12 as well as the regulatory cytokine IL-10. It is known that *L. amazonensis* infection modulates an organ-compartmentalized cytokine response in susceptible and

https://doi.org/10.1021/acs.jmedchem.1c00725
J. Med. Chem. 2021, 64, 12691−12704

resistant mice,[50] and *Leishmania* parasite elimination is accomplished with a robust pro-inflammatory response, accompanied by the release of host-protective cytokines.[51] The upregulation of cytokines that play a part in the inflammatory response in leishmaniasis observed in BALB/c peritoneal macrophages infected or not with *L. amazonensis* highlighted the *in vitro* immunomodulatory activity of compound **4** and its potential to enhance the immune response against *Leishmania* infection. Further studies should clarify the possible maintenance of this immunomodulation action in an experimental model *in vivo* and its role in the treatment of the disease.

The prediction of physicochemical, ADME (absorption, distribution, metabolism, and excretion) pharmacokinetics, and toxicity properties of the 1,2,3-triazole derivative compounds by *in silico* evaluation are important tools that can be incorporated in the development of desired characteristics that lead to optimization of drug discovery.[52] Thus, in addition to the *in vitro* antileishmanial activity, we also performed an *in silico* study of 1,2,3-triazole derivative compounds.

The compound that presented better overall results against *in vitro Leishmania* infection, compound **4**, also exhibited drug-likeness properties adequate to that of a hit compound, with no violation to Lipinski rules of five, Veber, Ghose, Egan, and Muegge methods. Pharmacokinetics properties of compound **4** demonstrated ADME prediction similar to or better than that of miltefosine. Toxicity prediction also revealed even better results than miltefosine, with compound **4** displaying no hepatotoxicity or skin sensibilization. The *in vitro* antileishmanial activity and the *in silico* prediction results allow us to classify compound **4** as a compound with promising potential and a candidate for conducting advanced studies for the development of drugs against leishmaniasis.

CONCLUSIONS

We verified the *in vitro* activity of 1,2,3-triazole derivative compounds against promastigotes and intracellular amastigotes of *L. amazonensis*. The 1,2,3-triazole derivative compounds were able to induce ultrastructural alterations in *L. amazonensis* promastigote forms. We also showed that compound **4** can increase the NO production by peritoneal macrophages and this increase plays a key role in its activity against *L. amazonensis* intracellular amastigotes. *In silico* prediction results in association with the antileishmanial activity revealed compound **4** as a hit compound with promising potential that will be evaluated in further studies.

EXPERIMENTAL SECTION

Reagents. The reagents Schneider's insect medium, streptomycin, DMSO, miltefosine, 3-(4,5-dimethylthiazol-2-yl)-2,5-diphenyltetrazolium bromide (MTT), Brewer thioglycollate medium, RPMI 1640 medium, xylol, acetone, glutaraldehyde, sodium-cacodylate, OsO_4, potassium ferrocyanide, $CaCl_2$, uranyl acetate, lead citrate, sodium citrate, sulfanilamide, *N*-(1-naphthyl)ethylenediamine, H_3PO_4, and 1400W were purchased from Sigma-Aldrich, St. Louis, MO, USA. Fetal bovine serum (FBS) and penicillin were purchased from Gibco, Gaithersburg, MD, USA. EMbed 812 resin was purchased from Electron Microscopy Sciences, Hatfield, PA, USA. Ketamine and xylazine were purchased from Syntec, Barueri, Brazil. Giemsa's azur-eosin-methylene blue and Entellan were purchased from Merck, Darmstadt, Germany. The TRIzol reagent was purchased from Invitrogen, Karlsruhe, Germany. The DNA-free DNA removal kit was purchased from Ambion, Carlsbad, CA, USA. The iScript cDNA synthesis kit was purchased from Bio-Rad Laboratories, Hercules, CA, USA. The GoTaq qPCR master mix was purchased from Promega, Madison, Wisconsin, USA.

1,2,3-Triazole Derivative Compound Synthesis. The synthesis of 1,2,3-triazole derivative compounds was carried out by the CuAAC reaction, as described previously by da Silva et al., 2020.[53] Structural elucidation was performed by high-resolution mass spectroscopy and nuclear magnetic resonance techniques (^{1}H NMR and ^{13}C NMR). Compounds are proven to be >95% pure by high-performance liquid chromatography (HPLC) analysis (additional details are given in Supporting Information Figure S1).

Parasites. Promastigote forms of *L. amazonensis* (MHOM/BR/76/MA-76), obtained from a human case of diffuse leishmaniasis and characterized by isoenzyme[54] and lectin techniques,[55] were cultured at 26 °C in Schneider's insect medium supplemented with 10% inactivated FBS, 100 U/mL penicillin, and 100 μg/mL streptomycin. Parasites with a maximum of five *in vitro* culture passages were used in the experiments.

Activity of 1,2,3-Triazole Derivative Compounds against *L. amazonensis* Promastigote Forms. An amount of 50 μL of *L. amazonensis* promastigote form culture in exponential growth at 2×10^6/mL was placed in a 96-well plate. Parasites were then incubated with 50 μL of 1,2,3-triazole derivative compounds or miltefosine at different concentrations (200−3.12 μM) at a final volume of 100 μL per well. The six concentrations assayed were obtained after a 1:100 dilution of the stock solution in DMSO to the highest concentration analyzed and posterior serial dilution 1:2 in the culture medium. Wells with parasites incubated with 50 μL of DMSO 1% or with 100 μL of the parasite-free medium was used as the control and blank, respectively. After 24 h incubation at 26 °C, the modified MTT viability assay was carried out as described elsewhere.[56] Briefly, 10 μL of the MTT solution at 5 mg/mL was added to each well, and after 5 h, 150 μL of DMSO was added. The plate was shaken in a shaker-plate for 15 min, and absorbance was read using the spectrophotometer EZ Read 400 (Biochrom, Cambridge, UK) at 570 nm. Absorbance values were normalized using the following formula: % viable parasites = (sample absorbance − blank absorbance)/(control absorbance − blank absorbance) × 100. The data were used to calculate the IC_{50} values.

Animals. Twelve BALB/c female mice 4−6 weeks old were provided by the Institute of Science and Technology in Biomodels (Instituto de Ciência e Tecnologia em Biomodelos), Instituto Oswaldo Cruz, Rio de Janeiro. The animals were maintained under pathogen-free conditions and handled following the recommendations of the National Council for Control of Animal Experimentation (Conselho Nacional de Controle de Experimentação Animal—CONCEA). The local Ethics Committee on Animal Care and Utilization approved all procedures involving the animals by the license number CEUA/IOC-L053/2016, granted on December 28, 2016.

Obtaining Peritoneal Macrophages and Culture. The BALB/c mice were inoculated intraperitoneally with 3 mL of sterile Brewer thioglycollate medium. After 72 h, animals were euthanized with a 250 μL intraperitoneal injection of a 1:1 mixture of ketamine (100 mg/mL) and xylazine (20 mg/mL). Peritoneal macrophages were harvested with 10 mL of chilled phosphate-buffered saline (PBS) pH 7.0, centrifuged at 1500 rpm for 15 min at 4 °C, suspended in RPMI 1640 medium with 10% inactivated FBS, 100 U/mL penicillin, and 100 μg/mL streptomycin, and immediately used in experiments incubated at 37 °C and 5% CO_2.

CCD-1072 Cell Culture. Human fibroblast cell line CCD-1072Sk (ATCC CRL-2088), taken from the normal foreskin of a neonate, was cultured in Iscove's modified Dulbecco's medium supplemented with 10% inactivated FBS, 100 U/mL penicillin, and 100 μg/mL streptomycin at 37 °C and 5% CO_2.

Cytotoxicity Assay. Peritoneal macrophages and CCD-1072Sk fibroblasts at 5×10^5 cells/mL, 100 μL per well, were cultured in a 96-well flat plate overnight at 37 °C and 5% CO_2. Then, the medium with nonadherent cells were carefully removed, and 100 μL of the new medium with different concentrations of 1,2,3-triazole derivative compounds or miltefosine (400−6.25 μM), obtained as described before, were added to wells with adherent cells. Wells with parasites incubated with 100 μL of DMSO 1% or with 100 μL of cell-free

https://doi.org/10.1021/acs.jmedchem.1c00725
J. Med. Chem. 2021, 64, 12691−12704

medium was used as the control and blank, respectively. After 24 h, the MTT viability assay was carried out.[57] Briefly, 10 μL of the MTT solution at 5 mg/mL was added to each well, the medium was completely removed after 2 h, and then, 100 μL of DMSO was added. The plate was shaken in a shaker-plate for 15 min to solubilize the formazan crystals, and absorbance and CC_{50} values were obtained as described before.

Activity of 1,2,3-Triazole Derivative Compounds against *L. amazonensis* Intracellular Amastigotes. Peritoneal macrophages at 10^6 cells/mL were cultured in a 24-well plate with coverslips, 500 μL per well, overnight at 37 °C and 5% CO_2. The medium with nonadherent cells was removed, and 1 mL of the medium with promastigote forms of *L. amazonensis* at 2×10^6 parasites/mL was added to each well, maintained at 35 °C and 5% CO_2 overnight. Then, the medium with noninternalized promastigotes was removed, and 1 mL of the medium with different concentrations of 1,2,3-triazole derivative compounds or miltefosine (40−2.5 μM) obtained as described before was added to wells. Wells with infected cells treated with DMSO at 0.5% were used as the control. After 24 h of treatment, coverslips with infected cells were fixed with Bouin solution, washed three times with PBS, stained with Giemsa's azur-eosin-methylene blue, dehydrated, diaphanized with solutions in increasing grades of acetone/xylol (100% acetone; 70:30, 50:50, 30:70% acetone/xylol; and 100% xylol), and mounted on a glass slide with Entellan. Intracellular amastigotes in 100 cells were counted by light microscopy, and data were normalized by the following formula: % intracellular amastigotes = sample count/control count × 100. The IC_{50} value for intracellular amastigotes was calculated as described before. The parameters of infection were calculated as described elsewhere.[58] The ratio of CC_{50} against IC_{50} for promastigotes or intracellular amastigotes was used to calculate the SI.

Transmission Electron Microscopy. Ultrastructural analysis was carried out with *L. amazonensis* promastigote forms treated for 24 h with the IC_{50} of 1,2,3-triazole derivative compounds. Transmission electron microscopy was performed as described elsewhere.[13] Briefly, the parasites were processed as follows: fixation with glutaraldehyde 2.5% in sodium-cacodylate buffer 0.1 M, pH 7.2 overnight; post-fixation in 1% OsO_4, 0.8% potassium ferrocyanide, and 5 mM $CaCl_2$; and dehydration in graded acetone and embedded in EMbed 812 resin. Ultrathin cuts of 100 nm, obtained in a Sorvall MT 2-B (Porter Blum) ultramicrotome (Sorvall, Newtown, CT, USA), were stained with 5% uranyl acetate aqueous solution and lead citrate (1.33% lead nitrate and 1.76% sodium citrate) and examined in a transmission electron microscope JEM-1011 (JEOL, Tokyo, Japan) operating at 80 kV.

NO Production in *L. amazonensis*-Stimulated Peritoneal Macrophages Treated with 1,2,3-Triazole Derivative Compounds. First, we performed an experiment without *L. amazonensis* stimulation to define the better concentration of 1,2,3-triazole derivative compound treatment that induces NO production. BALB/c peritoneal macrophages at 5×10^6 cells/mL were cultured in a 96-well plate, 100 μL per well, overnight at 37 °C and 5% CO_2. The medium with nonadherent cells was removed, and 100 μL of the medium with the 1,2,3-triazole derivative compound **4** at 5, 50, or 100 μM or lipopolysaccharide (LPS) at 10 μg/mL was added to each well. After 48 h, the supernatant was removed and used to carry out the nitrite quantification by the Griess reaction,[59] and 100 μL of the medium with 10 μL of the MTT solution (5 mg/mL) was added to each well to access cell viability as described before. Then, *L. amazonensis* stimulation protocols were carried out. Cells at 5×10^6 cells/mL were cultured in a 96-well plate as described before, and stimulation was achieved with *L. amazonensis* promastigotes at a 4:1 parasite/cell proportion or LPS at 10 μg/mL. After 1 h, *L. amazonensis*-stimulated cells were treated with compound **4** for 48 h at 37 °C and 5% CO_2, at a concentration that presented unaltered cell viability and enhanced nitrite quantification. The supernatant of stimulated cells was used to quantify nitrite by the Griess reaction, and cells were submitted to total RNA extraction for iNOS and cytokines mRNA quantification.

Nitrite Quantification. Nitrite quantification was used to indirectly quantify NO and was performed by the Griess assay[59] with modifications. Briefly, 50 μL of the culture supernatant was added to 50 μL of the Griess reagent [25 μL of sulfanilamide 1% in 2.5% H_3PO_4 solution and 25 μL of *N*-(1-naphthyl)ethylenediamine 0.1% solution] in 96-well plates. A standard curve of $NaNO_2$ with 100−0.3 μM was obtained by 1:2 serial dilution in triplicate, and the blank with only medium was also analyzed. After being protected for 10 min from light, the plate absorbance was read at 570 nm on the spectrophotometer EZ Read 400. The absorbance values of samples were subtracted from those of the blank and then transformed in $NaNO_2$ μM concentration according to the standard curve linear regression fit. The results were described as $NaNO_2$ μM in 5×10^6 cells/mL.[60]

Quantification of iNOS and Cytokines mRNA Expression by Real-Time Polymerase Chain Reaction. Total RNA extraction was performed with the TRIzol reagent. RNA was submitted to DNAse treatment and removal with a DNA-free DNA removal kit and quantified with Nanodrop One (Applied Biosystems, Waltham, MA, USA). The complementary DNA (cDNA) synthesis was carried out with 1 μg of total RNA using the iScript cDNA synthesis kit following the manufacturer's instructions. Primers targeting the genes iNOS, TNF-α, IL-1β, IL-6, IL-12, and IL-10 and the endogene RPLP0 (ribosomal protein lateral stalk subunit P0) were manufactured by Invitrogen (Table S5). The quantitative real-time polymerase chain reaction (qPCR) assays were performed in 96-well plates at a final volume of 10 μL per well, with 5 μL of the GoTaq qPCR master mix, 0.5 μL each of forward and reverse primer at 100 nM for each target, 2 μL of cDNA at 80 ng/μL or water (negative control reaction), and 2 μL of ultra-pure water. Reactions were run in a QuantStudio 3 RT-PCR system (Applied Biosystems, Waltham, MA, USA) with the fast run mode parameters as follows: a hold at 95 °C for 2 min, followed by 40 cycles of 95 °C for 3 s and 60 °C for 30 s, a melt curve stage of 95 °C for 1 s and 60 °C for 20 s, and a dissociation step of 0.1 °C/s up to 95 °C for 1 s. The results were analyzed with QuantStudio Design and Analysis Software v1.5.0 (Applied Biosystems, Waltham, MA, USA). The iNOS relative quantification was calculated by a comparative $2^{-\Delta\Delta C_t}$ method using the gene RPLP0 as the endogenous control.[20]

iNOS Inhibition in *L. amazonensis*-Stimulated Peritoneal Macrophages Treated with 1,2,3-Triazole Derivative Compounds. BALB/c peritoneal macrophages were cultured in a 96-well plate as described before and pretreated with 1400W,[21] a selective iNOS inhibitor, at 200 nM for 1 h. Then, cells were stimulated with *L. amazonensis* or LPS and treated with compound **4** for 48 h at 37 °C and 5% CO_2 as described before. The supernatants of the cultures were collected to carry out the nitrite quantification as described before.

iNOS Inhibition in Peritoneal Macrophages Infected with *L. amazonensis* and Treated with 1,2,3-Triazole Derivative Compounds. The infection protocol was followed as described before with some modifications. In brief, BALB/c peritoneal macrophages were cultured in a 24-well plate, pretreated with 1400W at 200 nM for 1 h, infected with *L. amazonensis,* and treated with compound **4** at 37 °C and 5% CO_2. After 24 h of treatment, coverslips with cells were submitted to staining processing, and analysis of the parameters of infection was conducted as described before.

***In Silico* Physicochemical and Pharmacokinetics Prediction of 1,2,3-Triazole Derivative Compounds.** The single database file of the simplified molecular input line entry system (SMILES) of the structures of the 1,2,3-triazole derivative compounds was obtained using ChemDraw software (version Ultra 12.0, PerkinElmer Informatics, Waltham, MA, USA). *In silico* physicochemical, drug-likeness, pharmacokinetics, and toxicity properties were predicted with the pkCSM[61] and SwissADME[62] web tools.

Statistical Analysis. Data are expressed as mean ± standard deviation (SD) in tables or plotted in graphs. The IC_{50} and CC_{50} values were calculated from the nonlinear regression curve fit of the log of the inhibitor concentration versus the normalized response of parasites or cell viability. The standard curve linear regression fit of $NaNO_2$ was obtained from a known concentration of the standard curve versus absorbance values using a standard curve linear regression fit with $R^2 > 0.99$. Differences between groups were analyzed by the Kruskal−Wallis test, followed by multiple comparison Dunn's test, or by the Mann−Whitney test, considering a significance level of 5%. Statistical analysis

https://doi.org/10.1021/acs.jmedchem.1c00725
J. Med. Chem. 2021, 64, 12691−12704

was conducted and graphs were obtained using software GraphPad Prism 7.00 (GraphPad Software, San Diego, CA, USA).

■ ASSOCIATED CONTENT

Supporting Information

The Supporting Information is available free of charge at https://pubs.acs.org/doi/10.1021/acs.jmedchem.1c00725.

In silico predictions of physicochemical, drug-likeness, pharmacokinetics, and toxicity properties of 1,2,3-triazole derivative compounds, sequence primers of iNOS and cytokines used for RT-PCR, and HPLC chromatogram of compound **4** (PDF)

Molecular formula strings of 1,2,3-triazole derivative compounds (CSV)

■ AUTHOR INFORMATION

Corresponding Authors

Fernando Almeida-Souza − *Laboratório de Anatomopatologia, Departamento de Patologia, Universidade Estadual do Maranhão, 65055-310 São Luís, Maranhão, Brazil; Laboratório de Imunomodulação e Protozoologia, Instituto Oswaldo Cruz, Fiocruz, 21040-900 Rio de Janeiro, Brazil;* orcid.org/0000-0003-0047-6159; Email: fernandoalsouza@gmail.com

Kátia da Silva Calabrese − *Laboratório de Imunomodulação e Protozoologia, Instituto Oswaldo Cruz, Fiocruz, 21040-900 Rio de Janeiro, Brazil;* orcid.org/0000-0002-1884-3765; Email: calabrese@ioc.fiocruz.br

Authors

Verônica Diniz da Silva − *Laboratório de Síntese Orgânica, Pontifícia Universidade Católica, 22451-900 Rio de Janeiro, Rio de Janeiro, Brazil*

Noemi Nosomi Taniwaki − *Núcleo de Microscopia Eletrônica, Instituto Adolfo Lutz, 01246-000 São Paulo, São Paulo, Brazil*

Daiana de Jesus Hardoim − *Laboratório de Imunomodulação e Protozoologia, Instituto Oswaldo Cruz, Fiocruz, 21040-900 Rio de Janeiro, Brazil*

Ailésio Rocha Mendonça Filho − *Laboratório de Anatomopatologia, Departamento de Patologia, Universidade Estadual do Maranhão, 65055-310 São Luís, Maranhão, Brazil*

Wendel Fragoso de Freitas Moreira − *Laboratório de Anatomopatologia, Departamento de Patologia, Universidade Estadual do Maranhão, 65055-310 São Luís, Maranhão, Brazil*

Camilla Djenne Buarque − *Laboratório de Síntese Orgânica, Pontifícia Universidade Católica, 22451-900 Rio de Janeiro, Rio de Janeiro, Brazil*

Ana Lucia Abreu-Silva − *Laboratório de Anatomopatologia, Departamento de Patologia, Universidade Estadual do Maranhão, 65055-310 São Luís, Maranhão, Brazil*

Complete contact information is available at: https://pubs.acs.org/10.1021/acs.jmedchem.1c00725

Author Contributions

K.d.S.C. and A.L.A.-S. contributed equally to this work. Conceptualization: F.A.-S., V.D.d.S., C.D.B., K.d.S.C., and A.L.A.-S.; chemistry: V.D.d.S. and C.D.B.; biology: F.A.-S., N.N.T., and D.d.J.H.; *in silico* data: A.R.M.F. and W.F.d.F.M.; writing: F.A.-S. and V.D.d.S.; and funding acquisition, C.D.B., K.d.S.C., and A.L.A.-S. All authors have given approval to the final version of the manuscript.

Notes

The authors declare no competing financial interest.

■ ACKNOWLEDGMENTS

This research was funded by the Coordination for the Improvement of Higher Education Personnel (Coordenação de Aperfeiçoamento de Pessoal de Nível Superior do Brazil; CAPES) grant number Finance Code 001 and the Carlos Chagas Filho Foundation for Research Support of the State of Rio de Janeiro (Fundação Carlos Chagas Filho de Amparo à Pesquisa do Estado do Rio de Janeiro; FAPERJ) grant number E-26/010.001759/2019. The Found for Conjoint Research Project (APC) was funded by the Oswaldo Cruz Institute (Instituto Oswaldo Cruz). Dr. F.A.-S. has a postdoctoral research fellowship with the CAPES grant number 88887.363006/2019-00. Dr. A.L.A.-S. has a research productivity fellowship of the National Scientific and Technological Development Council (Conselho Nacional de Desenvolvimento Científico e Tecnológico; CNPq) with the grant number 309885/2017-5.

■ ABBREVIATIONS

1400W, *N*-(3-(aminomethyl)benzyl)acetamidine dihydrochloride; AMES, *Salmonella*/microsome mutagenicity assay; BBB, blood−brain barrier; CC_{50}, 50% cytotoxicity concentration; cDNA, complementary DNA; CuAAC, copper-catalyzed alkyne−azide cycloaddition; DMSO, dimethyl sulfoxide; DNDi, Drugs for Neglected Diseases Initiative; eNOS, endothelial nitric oxide synthase; FBS, fetal bovine serum; hERG, human ether-a-go-go; HIA, human intestinal absorption; HIV, human immunodeficiency virus; HRMS, high-resolution mass spectroscopy; IC_{50}, 50% inhibitory concentration; IL, interleukin; iNOS, inducible nitric oxide synthase; LPS, lipopolysaccharide; MTT, 3-(4,5-dimethylthiazol-2-yl)-2,5-diphenyltetrazolium bromide; NO, nitric oxide; nNOS, neuronal nitric oxide synthase; OCT2, organic cation transporter 2; PAINS, pan-assay interference compounds; PBS, phosphate-buffered saline; PGP, P-glycoprotein; RPLP0, ribosomal protein lateral stalk subunit P0; RQ, relative quantification; RT-PCR, real-time polymerase chain reaction; SI, selectivity index; SI_{ama}, selectivity index for intracellular amastigote; SI_{pro}, selectivity index for promastigote; SMILES, simplified molecular input line entry system; TNF-α, tumor necrosis factor α

■ REFERENCES

(1) Braga, S. S. Multi-target drugs active against leishmaniasis: A paradigm of drug repurposing. *Eur. J. Med. Chem.* **2019**, *183*, 111660.

(2) de Macedo-Silva, S. T.; de Souza, W.; Rodrigues, J. C. F. Sterol biosynthesis pathway as an alternative for the anti-protozoan parasite chemotherapy. *Curr. Med. Chem.* **2015**, *22*, 2186−2198.

(3) WHO. *Control of the Leishmaniases: Report of a Meeting of the WHO Expert Committee on the Control of Leishmaniasis, Geneva, Switzerland, 2010*; World Health Organization: Geneva, 2010; p 202.

(4) Dheer, D.; Singh, V.; Shankar, R. Medicinal attributes of 1,2,3-triazoles: current developments. *Bioorg. Chem.* **2017**, *71*, 30−54.

(5) Kolb, H. C.; Sharpless, K. B. The growing impact of click chemistry on drug discovery. *Drug Discovery Today* **2003**, *8*, 1128−1137.

(6) Bonandi, E.; Christodoulou, M. S.; Fumagalli, G.; Perdicchia, D.; Rastelli, G.; Passarella, D. The 1,2,3-triazole ring as a bioisostere in medicinal chemistry. *Drug Discovery Today* **2017**, *22*, 1572−1581.

(7) Swetha, Y.; Reddy, E. R.; Kumar, J. R.; Trivedi, R.; Giribabu, L.; Sridhar, B.; Rathod, B.; Prakasham, R. S. Synthesis, characterization and

antimicrobial evaluation of ferrocene−oxime ether benzyl 1H-1,2,3-triazole hybrids. *New J. Chem.* **2019**, *43*, 8341−8351.
(8) Song, M.-X.; Deng, X.-Q. Recent developments on triazole nucleus in anticonvulsant compounds: a review. *J. Enzyme Inhib. Med. Chem.* **2018**, *33*, 453−478.
(9) Mohammed, I.; Kummetha, I. R.; Singh, G.; Sharova, N.; Lichinchi, G.; Dang, J.; Stevenson, M.; Rana, T. M. 1,2,3-Triazoles as amide bioisosteres: discovery of a new class of potent hiv-1 vif antagonists. *J. Med. Chem.* **2016**, *59*, 7677−7682.
(10) Yadav, P.; Lal, K.; Kumar, A.; Guru, S. K.; Jaglan, S.; Bhushan, S. Green synthesis and anticancer potential of chalcone linked-1,2,3-triazoles. *Eur. J. Med. Chem.* **2017**, *126*, 944−953.
(11) Dasari, S. R.; Tondepu, S.; Vadali, L. R.; Seelam, N. Design, synthesis and molecular modeling of nonsteroidal anti-inflammatory drugs tagged substituted 1,2,3-triazole derivatives and evaluation of their biological activities. *J. Heterocycl. Chem.* **2019**, *56*, 1318−1329.
(12) Meinel, R. S.; Almeida, A. D. C.; Stroppa, P. H. F.; Glanzmann, N.; Coimbra, E. S.; da Silva, A. D. Novel functionalized 1,2,3-triazole derivatives exhibit antileishmanial activity, increase in total and mitochondrial-ros and depolarization of mitochondrial membrane potential of *Leishmania amazonensis*. *Chem.-Biol. Interact.* **2020**, *315*, 108850.
(13) Almeida-Souza, F.; da Silva, V. D.; Silva, G. X.; Taniwaki, N. N.; Hardoim, D. d. J.; Buarque, C. D.; Abreu-Silva, A. L.; Calabrese, K. d. S. 1,4-disubstituted-1,2,3-triazole compounds induce ultrastructural alterations in *Leishmania amazonensis* promastigote: an in vitro antileishmanial and in silico pharmacokinetic study. *Int. J. Mol. Sci.* **2020**, *21*, 6839.
(14) Pertino, M. W.; F de la Torre, A.; Schmeda-Hirschmann, G.; Vega, C.; Rolón, M.; Coronel, C.; Rojas de Arias, A.; Leal López, K.; Carranza-Rosales, P.; Viveros Valdez, E. Synthesis, trypanocidal and anti-leishmania activity of new triazole-lapachol and nor-lapachol hybrids. *Bioorg. Chem.* **2020**, *103*, 104122.
(15) Sasidharan, S.; Saudagar, P. Leishmaniasis: where are we and where are we heading? *Parasitol. Res.* **2021**, *120*, 1541−1554.
(16) Capela, R.; Moreira, R.; Lopes, F. An overview of drug resistance in protozoal diseases. *Int. J. Mol. Sci.* **2019**, *20*, 5748.
(17) Barral, A.; Pedral-Sampaio, D.; Grimaldi, G., Jr.; Momen, H.; McMahon-Pratt, D.; Ribeiro de Jesus, A.; Almeida, R.; Badaro, R.; Barral-Netto, M.; Carvalho, E. M.; Johnson, W. D., Jr. Leishmaniasis in Bahia, Brazil: evidence that *Leishmania amazonensis* produces a wide spectrum of clinical disease. *Am. J. Trop. Med. Hyg.* **1991**, *44*, 536−546.
(18) Azim, M.; Khan, S. A.; Ullah, S.; Ullah, S.; Anjum, S. I. Therapeutic advances in the topical treatment of cutaneous leishmaniasis: a review. *PLoS Neglected Trop. Dis.* **2021**, *15*, No. e0009099.
(19) Akbari, M.; Oryan, A.; Hatam, G. Immunotherapy in treatment of leishmaniasis. *Immunol. Lett.* **2021**, *233*, 80−86.
(20) Almeida-Souza, F.; Cardoso, F. d. O.; Souza, B. V. d. C.; do Valle, T. Z.; de Sá, J. C.; Oliveira, I. d. S. d. S.; de Souza, C. d. S. F.; Moragas Tellis, C. J.; Chagas, M. d. S. d. S.; Behrens, M. D.; Abreu-Silva, A. L.; Calabrese, K. d. S. *Morinda citrifolia* Linn. Reduces parasite load and modulates cytokines and extracellular matrix proteins in C57BL/6 mice infected with *Leishmania (Leishmania) amazonensis*. *PLoS Neglected Trop. Dis.* **2016**, *10*, No. e0004900.
(21) Almeida-Souza, F.; de Souza, C. d. S. F.; Taniwaki, N. N.; Silva, J. J. M.; de Oliveira, R. M.; Abreu-Silva, A. L.; Calabrese, K. d. S. *Morinda citrifolia* Linn. fruit (Noni) juice induces an increase in NO production and death of *Leishmania amazonensis* amastigotes in peritoneal macrophages from BALB/c. *Nitric Oxide* **2016**, *58*, 51−58.
(22) Roatt, B. M.; de Oliveira Cardoso, J. M.; De Brito, R. C. F.; Coura-Vital, W.; de Oliveira Aguiar-Soares, R. D.; Reis, A. B. Recent advances and new strategies on leishmaniasis treatment. *Appl. Microbiol. Biotechnol.* **2020**, *104*, 8965−8977.
(23) Stroppa, P. H. F.; Antinarelli, L. M. R.; Carmo, A. M. L.; Gameiro, J.; Coimbra, E. S.; da Silva, A. D. Effect of 1,2,3-triazole salts, non-classical bioisosteres of miltefosine, on *Leishmania amazonensis*. *Bioorg. Med. Chem.* **2017**, *25*, 3034−3045.
(24) Auffinger, P.; Hays, F. A.; Westhof, E.; Ho, P. S. Halogen bonds in biological molecules. *Proc. Natl. Acad. Sci. U.S.A.* **2004**, *101*, 16789−16794.
(25) Odlo, K.; Fournier-Dit-Chabert, J.; Ducki, S.; Gani, O. A.; Sylte, I.; Hansen, T. V. 1,2,3-triazole analogs of combretastatin A-4 as potential microtubule-binding agents. *Bioorg. Med. Chem.* **2010**, *18*, 6874−6885.
(26) Ellouz, M.; Sebbar, N. K.; Fichtali, I.; Ouzidan, Y.; Mennane, Z.; Charof, R.; Mague, J. T.; Urrutigoïty, M.; Essassi, E. M. Synthesis and antibacterial activity of new 1,2,3-triazolylmethyl-2H-1,4-benzothiazin-3(4H)-one derivatives. *Chem. Cent. J.* **2018**, *12*, 123.
(27) Cassamale, T. B.; Costa, E. C.; Carvalho, D. B.; Cassemiro, N. S.; Tomazela, C. C.; Marques, M. C. S.; Ojeda, M.; Matos, M. F. C.; Albuquerque, S.; Arruda, C. C. P.; Baroni, A. C. M. Synthesis and antitrypanosomastid activity of 1,4-diaryl-1,2,3-triazole analogues of neolignans veraguensin, grandisin and machilin G. *J. Braz. Chem. Soc.* **2016**, *27*, 1217−1228.
(28) Jiang, S.; Zhang, L.; Cui, D.; Yao, Z.; Gao, B.; Lin, J.; Wei, D. The important role of halogen bond in substrate selectivity of enzymatic catalysis. *Sci. Rep.* **2016**, *6*, 34750.
(29) Rodrigues, J. C. F.; Attias, M.; Rodriguez, C.; Urbina, J. A.; de Souza, W. Ultrastructural and biochemical alterations induced by 22,26-azasterol, a delta(24(25))-sterol methyltransferase inhibitor, on promastigote and amastigote forms of *Leishmania amazonensis*. *Antimicrob. Agents Chemother.* **2002**, *46*, 487−499.
(30) Tiuman, T. S.; Ueda-Nakamura, T.; Garcia Cortez, D. A.; Dias Filho, B. P.; Morgado-Díaz, J. A.; de Souza, W.; Nakamura, C. V. Antileishmanial activity of parthenolide, a sesquiterpene lactone isolated from *Tanacetum parthenium*. *Antimicrob. Agents Chemother.* **2005**, *49*, 176−182.
(31) Teixeira de Macedo Silva, S.; Visbal, G.; Lima Prado Godinho, J.; Urbina, J. A.; de Souza, W.; Cola Fernandes Rodrigues, J. In vitro antileishmanial activity of ravuconazole, a triazole antifungal drug, as a potential treatment for leishmaniasis. *J. Antimicrob. Chemother.* **2018**, *73*, 2360−2373.
(32) Holanda, V. N.; da Silva, W. V.; do Nascimento, P. H.; Silva, S. R. B.; Cabral Filho, P. E.; de Oliveira Assis, S. P.; da Silva, C. A.; de Oliveira, R. N.; de Figueiredo, R. C. B. Q.; de Menezes Lima, V. L. Antileishmanial activity of 4-phenyl-1-[2-(phthalimido-2-yl)ethyl]-1H-1,2,3-triazole (PT4) derivative on *Leishmania amazonensis* and *Leishmania braziliensis*: In silico ADMET, in vitro activity, docking and molecular dynamic simulations. *Bioorg. Chem.* **2020**, *105*, 104437.
(33) Olivier, V.; Duval, J.-L.; Hindié, M.; Pouletaut, P.; Nagel, M. D. Comparative particle-induced cytotoxicity toward macrophages and fibroblasts. *Cell Biol. Toxicol.* **2003**, *19*, 145−159.
(34) Moura, C. C. G.; Oliveira, N. C. M.; Borges, C. R. B.; de Souza, M. A.; Biffi, J. C. G. Cytotoxic response of two cell lines exposed in vitro to four endodontic sealers. *Braz. J. Oral Sci.* **2012**, *11*, 135−140.
(35) Boechat, N.; Pinto, A. d. C.; Bastos, M. M. Métodos seletivos de fluoração de moléculas orgânicas. *Quím. Nova* **2015**, *38*, 1323−1338.
(36) Limban, C.; Chifiriuc, M. C.; Caproiu, M. T.; Dumitrascu, F.; Ferbinteanu, M.; Pintilie, L.; Stefaniu, A.; Vlad, I. M.; Bleotu, C.; Marutescu, L. G.; Nuta, D. C. New substituted benzoylthiourea derivatives: from design to antimicrobial applications. *Molecules* **2020**, *25*, 1478.
(37) Ioset, J.; Brun, R.; Wenzler, T.; Kaiser, M.; Yardley, V. *Drug Screening for Kinetoplastid Diseases: A Training Manual for Screening in Neglected Diseases*; DNDi, 2009; p 74.
(38) Katsuno, K.; Burrows, J. N.; Duncan, K.; van Huijsduijnen, R. H.; Kaneko, T.; Kita, K.; Mowbray, C. E.; Schmatz, D.; Warner, P.; Slingsby, B. T. Hit and lead criteria in drug discovery for infectious diseases of the developing world. *Nat. Rev. Drug Discovery* **2015**, *14*, 751−758.
(39) Damasceno-Sá, J. C.; de Souza, F. S.; Dos Santos, T. A. T.; de Oliveira, F. C.; da Silva, M. d. F. S.; Dias, R. R. F.; de Souza, W.; Arnholdt, A. C. V.; Seabra, S. H.; DaMatta, R. A. Inhibition of nitric oxide production of activated mice peritoneal macrophages is independent of the *Toxoplasma gondii* strain. *Mem. Inst. Oswaldo Cruz* **2021**, *116*, No. e200417.

https://doi.org/10.1021/acs.jmedchem.1c00725
J. Med. Chem. 2021, 64, 12691−12704

(40) Fang, W.; Jiang, J.; Su, L.; Shu, T.; Liu, H.; Lai, S.; Ghiladi, R. A.; Wang, J. The role of NO in COVID-19 and potential therapeutic strategies. *Free Radical Biol. Med.* **2021**, *163*, 153−162.
(41) Badirzadeh, A.; Montakhab-Yeganeh, H.; Miandoabi, T. Arginase/nitric oxide modifications using live non-pathogenic *Leishmania tarentolae* as an effective delivery system inside the mammalian macrophages. *J. Parasit. Dis.* **2021**, *45*, 65−71.
(42) Kupani, M.; Sharma, S.; Pandey, R. K.; Kumar, R.; Sundar, S.; Mehrotra, S. IL-10 and TGF-β Induced arginase expression contributes to deficient nitric oxide response in human visceral leishmaniasis. *Front. Cell. Infect. Microbiol.* **2021**, *10*, 614165.
(43) Fang, F. C. Antimicrobial reactive oxygen and nitrogen species: concepts and controversies. *Nat. Rev. Microbiol.* **2004**, *2*, 820−832.
(44) Zheng, Y.; Zhang, Y.-l.; Li, Z.; Shi, W.; Ji, Y.-r.; Guo, Y.-H.; Huang, C.; Sun, G.-p.; Li, J. Design and synthesis of 7-O-1,2,3-triazole hesperetin derivatives to relieve inflammation of acute liver injury in mice. *Eur. J. Med. Chem.* **2021**, *213*, 113162.
(45) Li, S.-M.; Tsai, S.-E.; Chiang, C.-Y.; Chung, C.-Y.; Chuang, T.-J.; Tseng, C.-C.; Jiang, W.-P.; Huang, G.-J.; Lin, C.-Y.; Yang, Y.-C.; Fuh, M.-T.; Wong, F.-F. New methyl 5-(halomethyl)-1-aryl-1H-1,2,4-triazole-3-carboxylates as selective COX-2 inhibitors and anti-inflammatory agents: design, synthesis, biological evaluation, and docking study. *Bioorg. Chem.* **2020**, *104*, 104333.
(46) Kaoud, T. S.; Mohassab, A. M.; Hassan, H. A.; Yan, C.; Van Ravenstein, S. X.; Abdelhamid, D.; Dalby, K. N.; Abdel-Aziz, M. NO-releasing STAT3 inhibitors suppress BRAF-mutant melanoma growth. *Eur. J. Med. Chem.* **2020**, *186*, 111885.
(47) Mattila, J. T.; Thomas, A. C. Nitric oxide synthase: non-canonical expression patterns. *Front. Immunol.* **2014**, *5*, 478.
(48) Bredt, D. S. Endogenous nitric oxide synthesis: biological functions and pathophysiology. *Free Radical Res.* **1999**, *31*, 577−596.
(49) Garvey, E. P.; Oplinger, J. A.; Furfine, E. S.; Kiff, R. J.; Laszlo, F.; Whittle, B. J.; Knowles, R. G. 1400W is a slow, tight binding, and highly selective inhibitor of inducible nitric-oxide synthase in vitro and in vivo. *J. Biol. Chem.* **1997**, *272*, 4959−4963.
(50) Cardoso, F. d. O.; Zaverucha-do-Valle, T.; Almeida-Souza, F.; Abreu-Silva, A. L.; Calabrese, K. d. S. Modulation of cytokines and extracellular matrix proteins expression by *Leishmania amazonensis* in susceptible and resistant mice. *Front. Microbiol.* **2020**, *11*, 1986.
(51) Ghosh, S.; Roy, K.; Rajalingam, R.; Martin, S.; Pal, C. Cytokines in the generation and function of regulatory T cell subsets in leishmaniasis. *Cytokine* **2020**, 155266.
(52) de Souza Neto, L. R.; Moreira-Filho, J. T.; Neves, B. J.; Maidana, R. L. B. R.; Guimarães, A. C. R.; Furnham, N.; Andrade, C. H.; Silva, F. P. In silico strategies to support fragment-to-lead optimization in drug discovery. *Front. Chem.* **2020**, *8*, 93.
(53) da Silva, V. D.; Silva, R. R.; Gonçalves Neto, J.; López-Corcuera, B.; Guimarães, M. Z.; Noël, F.; Buarque, C. D. New α-hydroxy-1,2,3-triazoles and 9H-fluorenes-1,2,3-triazoles: synthesis and evaluation as glycine transporter 1 inhibitors. *J. Braz. Chem. Soc.* **2020**, *31*, 1258−1269.
(54) Grimaldi, G., Jr.; Momen, H.; Naiff, R. D.; McMahon-Pratt, D.; Barrett, T. V. Characterization and classification of leishmanial parasites from humans, wild mammals, and sand flies in the Amazon region of Brazil. *Am. J. Trop. Med. Hyg.* **1991**, *44*, 645−661.
(55) Schottelius, J.; Gonçalves da Costa, S. C. Studies on the relationship between lectin binding carbohydrates and different strains of *Leishmania* from the New World. *Mem. Inst. Oswaldo Cruz* **1982**, *77*, 19−27.
(56) Almeida-Souza, F.; Taniwaki, N. N.; Amaral, A. C. F.; de Souza, C. d. S. F.; Calabrese, K. d. S.; Abreu-Silva, A. L. Ultrastructural changes and death of *Leishmania infantum* promastigotes induced by *Morinda citrifolia* Linn. fruit (noni) juice treatment. *J. Evidence-Based Complementary Altern. Med.* **2016**, *2016*, 5063540.
(57) Mosmann, T. Rapid colorimetric assay for cellular growth and survival: application to proliferation and cytotoxicity assays. *J. Immunol. Methods* **1983**, *65*, 55−63.
(58) Oliveira, I. d. S. d. S.; Moragas Tellis, C. J.; Chagas, M. d. S. d. S.; Behrens, M. D.; Calabrese, K. d. S.; Abreu-Silva, A. L.; Almeida-Souza, F. *Carapa guianensis* Aublet (andiroba) seed oil: chemical composition and antileishmanial activity of limonoid-rich fractions. *BioMed Res. Int.* **2018**, *2018*, 5032816.
(59) Green, L. C.; Wagner, D. A.; Glogowski, J.; Skipper, P. L.; Wishnok, J. S.; Tannenbaum, S. R. Analysis of nitrate, nitrite, and [15N]nitrate in biological fluids. *Anal. Biochem.* **1982**, *126*, 131−138.
(60) Oliveira, I. d. S. d. S.; Colares, A. V.; Cardoso, F. d. O.; Tellis, C. J. M.; Chagas, M. d. S. d. S.; Behrens, M. D.; Calabrese, K. d. S.; Almeida-Souza, F.; Abreu-Silva, A. L. *Vernonia Polysphaera* Baker: Anti-inflammatory activity in vivo and inhibitory effect in LPS-stimulated RAW 264.7 cells. *PLoS One* **2019**, *14*, No. e0225275.
(61) Pires, D. E. V.; Blundell, T. L.; Ascher, D. B. pkCSM: Predicting small-molecule pharmacokinetic and toxicity properties using graph-based signatures. *J. Med. Chem.* **2015**, *58*, 4066−4072.
(62) Daina, A.; Michielin, O.; Zoete, V. SwissADME: A free web tool to evaluate pharmacokinetics, drug-likeness and medicinal chemistry friendliness of small Molecules. *Sci. Rep.* **2017**, *7*, 42717.

https://doi.org/10.1021/acs.jmedchem.1c00725
J. Med. Chem. 2021, 64, 12691−12704